International Journal of Thermophysics, Vol. 26, No. 4, July 2005 (© 2005)
DOI: 10.1007/s10765-005-6682-z

Combined DSC and Pulse-Heating Measurements of Electrical Resistivity and Enthalpy of Tungsten, Niobium, and Titanium[1]

B. Wilthan,[2] C. Cagran,[2] and G. Pottlacher[2,3]

Measurements of thermophysical properties such as enthalpy, electrical resistivity, and specific heat capacity as a function of temperature starting from the solid state into the liquid phase for W, Nb, and Ti are presented in this work. An ohmic pulse-heating technique allows measurements of enthalpy and electrical resistivity from room temperature to the end of the stable liquid phase within 60 μs. The simultaneous optical measurement of temperature is limited by the fast pyrometers with an onset temperature of $T_{\min}$ = 1200–1500 K; below these temperatures, the fast pyrometers are not sensitive. A differential scanning calorimeter (DSC) is used for determination of the specific heat capacity, and also to obtain enthalpy values in the temperature range of 600–1700 K. Combining the two methods entends the range of values of electrical resistivity and enthalpy versus temperature down to 600 K. Results on the metals W, Nb, and Ti are reported and compared to literature values. This paper is a continuation of earlier work.

KEY WORDS: differential scanning calorimetry; electrical resistivity; enthalpy; niobium; pulse-heating; specific heat; titanium; tungsten.

1. INTRODUCTION

Fast ohmic pulse heating of metals and alloys far into the liquid phase to obtain accurate thermophysical properties such as specific electrical resistivity and specific enthalpy as a function of temperature has been established

[1] Paper presented at the Seventh International Workshop on Subsecond Thermophysics, October 6–8, 2004, Orléans, France.

[2] Institute for Experimental Physics, Graz University of Technology, Petersgasse 16, 8010 Graz, Austria.

[3] To whom correspondence should be addressed. E-mail: pottlacher@tugraz.at

during the last twenty years in our laboratory [1, 2]. At the beginning, the interest was focused on data in the liquid phase of the material, as fast pyrometers with rise times of 100 ns had a relatively high onset temperature, whereas the electrical signals current, I, and voltage drop, V, which are used to obtain quantities like enthalpy or electrical resistivity, can be detected over the entire temperature range. The onset temperature of the pyrometers defines the lower limit for the range for which these quantities can be reported; this is a strong limitation. This issue has already been discussed extensively in Ref. 3. To overcome this limitation and to obtain temperature dependences for these quantities below the onset temperature of the pyrometers, a differential scanning calorimeter (Netzsch DSC 404) was added to our setup and incorporated into the basic measurement routines for data in the temperature range of about 500–1500 K. The DSC is basically designed and used for accurate specific-heat-capacity measurements in the above mentioned temperature range. The results are combined with those of the pulse-heating experiments by using the enthalpy (integrated c_p-values) versus temperature dependence of the DSC. Thus, temperature dependences of all thermophysical properties can now be extended down to the DSC onset temperature of about 500 K, and therefore reliable thermophysical data for the solid phase of the material under investigation are achieved.

2. MEASUREMENTS

During one fast pulse-heating experiment ($\sim$60 μs), we measure the current through the wire sample (which has an average 0.5 mm diameter and average 50 mm length), the voltage drop across it, and the radiation temperature. The temperatures covered by the different optical pyrometers range from 1200 K up to about 5000 K, depending on the actual emissivity of the material under investigation [3]. Thus, the lower temperature limit of the pyrometer of the pulse-heating experiment is also due to the use of a neutral density filter and reaches about 1700 K for titanium and niobium, and about 2300 K for tungsten.

In this work, the DSC is used for measurements of the heat capacity of the cylindrical sample (typical dimensions: 5.2 mm diameter, 0.5 mm length) in the temperature range from 500 K to the maximum of 1723 K for tungsten. The combination of pulse-heating experiments and DSC experiments enables an extension of the pulse-heating results for enthalpy versus temperature and resistivity versus temperature to lower temperature regions, starting at the onset temperature of the DSC (500 K). Up to now, our laboratory was unable to access these temperature regions by pure pyrometry. For further details on the experiment and data evaluation, see, e.g., Refs. 4 and 5.

3. RESULTS

The following melting temperatures have been used in the present work for data evaluation: tungsten: 3687 K [6], niobium: 2745 K [6], and titanium: 1943 K [6].

3.1. Tungsten

The tungsten wires for the experiments were fabricated by "Goodfellow Cambridge Ltd." with a nominal purity of 99.95%. The material for the cylindrical samples for the DSC-measurements were delivered by "Fa. Plansee GmbH" and cut from a plate in our machine shop. Additionally, we measured samples from the wire with no difference in value but in quality of signal because of the insufficient heat transfer to the probe.

In Fig. 1 the specific enthalpy versus temperature results are plotted for tungsten. In the temperature range from $423\,\mathrm{K} < T < 1723\,\mathrm{K}$, we obtain from our DSC measurements the following fit:

$$H(T) = -39.272 + 0.133T + 4.195 \times 10^{-6} T^2, \tag{1}$$

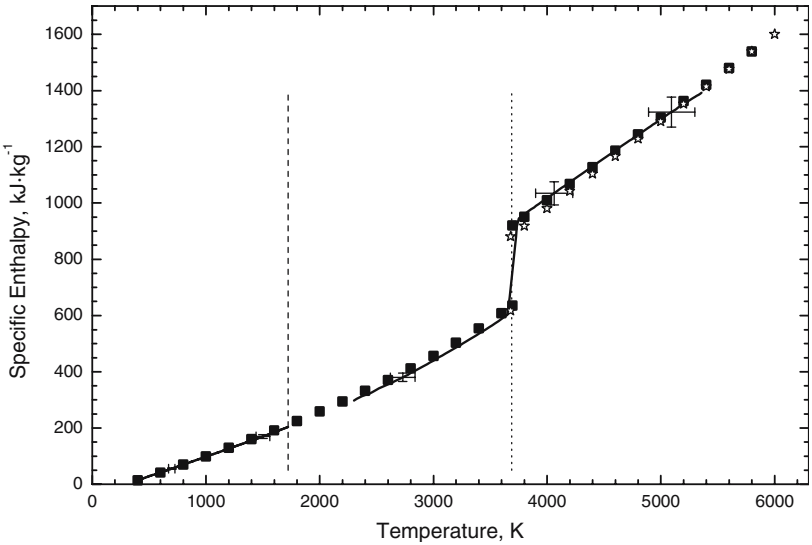

Fig. 1. Specific enthalpy versus temperature for tungsten. Bold solid lines represent measured data from this work; vertical dashed line: end of values measured and calculated with DSC data (1723 K); vertical dotted line: melting temperature (3687 K); filled squares: values of theoretical work from Gustafson [7]; and open stars: values from Seydel et al. [8].

where H is in $\mathrm{kJ\,kg^{-1}}$ and T is in K.

The linear fit for solid tungsten in the temperature range $2300\,\mathrm{K} < T < 3687\,\mathrm{K}$ is

$$H(T) = 83.342 + 0.011T + 3.576 \times 10^{-5} T^2, \tag{2}$$

For the liquid in the temperature range $3687\,\mathrm{K} < T < 5400\,\mathrm{K}$ we obtain

$$H(T) = -97.894 + 0.279T. \tag{3}$$

Figure 2 presents the specific electrical resistivity with the initial geometry ($\rho_{\mathrm{el,\ IG}}$, not compensated for thermal expansion) as a function of temperature for tungsten. In the temperature range from $423\,\mathrm{K} < T < 1723\,\mathrm{K}$ we obtain, combined with our DSC measurements, the following fit:

$$\rho_{\mathrm{el,IG}}(T) = -0.021 + 2.467 \times 10^{-4} T + 1.201 \times 10^{-8} T^2, \tag{4}$$

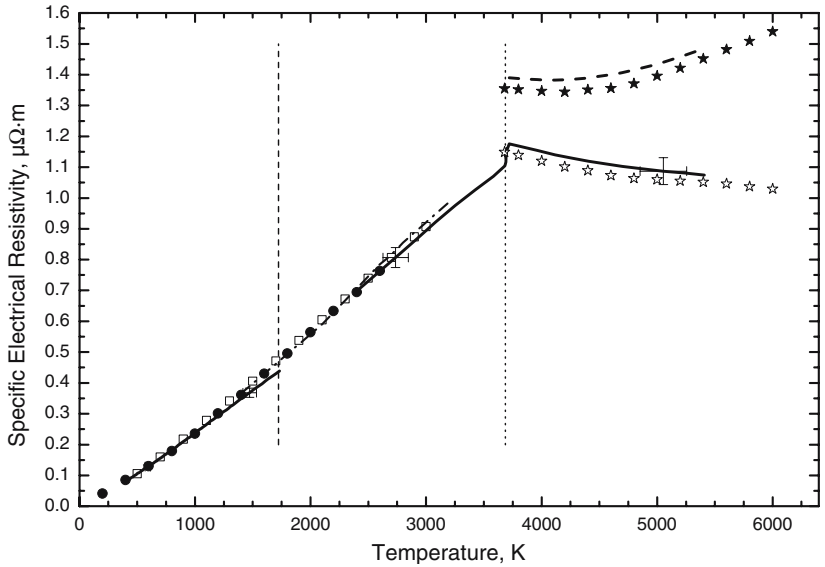

Fig. 2. Electrical resistivity of tungsten (with initial geometry) versus temperature. Bold solid line represents measured data from this work; bold dashed line: measured data, volume compensated; vertical dashed line: end of values measured and calculated with DSC data (1723 K); vertical dotted line: melting temperature (3687 K); filled circles: values from Goldsmith et al. [9] in the solid phase; dotted-dashed line: values from Zhorov [10]; open squares: values from Hust and Giarratano [11]; open stars: values from Seydel et al. [8] in the liquid phase; and filled stars: values from Seydel et al. [8] in the liquid phase (volume compensated).

where $\rho_{el,IG}$ is in $\mu\Omega$m and T is in K.

The linear fit to our values for the solid in the temperature range $2390\,K < T < 3687\,K$ is

$$\rho_{el,IG}(T) = -0.059 + 3.166 \times 10^{-4} T, \tag{5}$$

and for the liquid in the temperature range $3687\,K < T < 5400\,K$,

$$\rho_{el,IG}(T) = 1.833 - 2.573 \times 10^{-4} T + 2.169 \times 10^{-8} T^2. \tag{6}$$

The specific electrical resistivity with the volume expansion included, $\rho_{el,\,VOL}$, is depicted in Fig. 2 as a function of temperature for the liquid phase. The polynomial fit to our specific electrical resistivity with volume expansion included [8], $\rho_{el,\,VOL}$, in the temperature range $3687\,K < T < 5400\,K$ is

$$\rho_{el,VOL}(T) = 2.313 - 4.585 \times 10^{-4} T + 5.650 \times 10^{-8} T^2. \tag{7}$$

The effect of the volume expansion on resistivity is shown only for tungsten as an example. For all other materials only the resistivity at the initial geometry will be presented, as the compensation of volume expansion shifts the resistivity to higher values and can be done with the corresponding volume expansion data available in the literature.

3.2. Niobium

The wires used for the pulse-heating experiments were fabricated by "Goodfellow Cambridge Ltd." with a nominal purity of 99.9%. The cylindrical samples for the DSC-measurements were cut from a different single-crystal rod ([111]-2°).

Figure 3 presents the enthalpy versus temperature results for niobium. In the temperature range from $473\,K < T < 1573\,K$ we obtain from our DSC-measurements the following fit:

$$H(T) = -82.451 + 0.280T; \tag{8}$$

the linear fit for solid niobium obtained by pulse heating in the temperature range $1790\,K < T < 2745\,K$ is

$$H(T) = -248.023 + 0.380T; \tag{9}$$

and for the liquid in the temperature range $2745\,K < T < 3700\,K$,

$$H(T) = -129.387 + 0.466T. \tag{10}$$

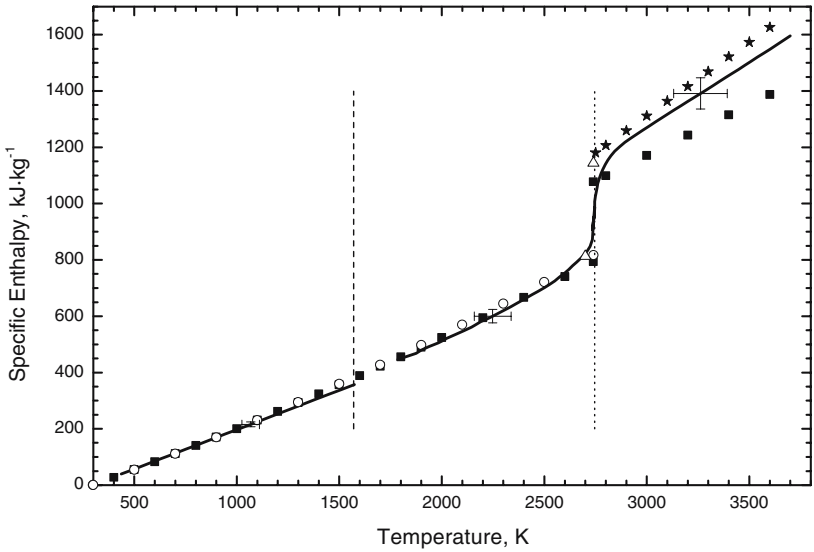

Fig. 3. Specific enthalpy versus temperature for niobium. Bold solid lines represent measured data from this work; vertical dashed line: end of values measured and calculated with DSC data (1570 K); vertical dotted line: melting temperature (2745 K); filled squares: values from Hultgren et al. [12]; open circles, values from Kirillin et al. [13]; open triangles: values from Sheindlin et al. [14]; and filled stars: values from Gallob et al. [15].

Figure 4 depicts the electrical resistivity with the initial geometry versus temperature for niobium.

In the range from $473\,\mathrm{K} < T < 1573\,\mathrm{K}$ we obtain, including the DSC-values,

$$\rho_{\mathrm{el,IG}}(T) = 0.023 + 4.839 \times 10^{-4} T - 8.899 \times 10^{-8} T^2, \tag{11}$$

By means of pulse heating, we obtain in the range $1790\,\mathrm{K} < T < 2745\,\mathrm{K}$,

$$\rho_{\mathrm{el,IG}}(T) = 0.199 + 2.441 \times 10^{-4} T, \tag{12}$$

and in the range $2745\,\mathrm{K} < T < 3700\,\mathrm{K}$,

$$\rho_{\mathrm{el,IG}}(T) = 0.972 + 5.527 \times 10^{-6} T. \tag{13}$$

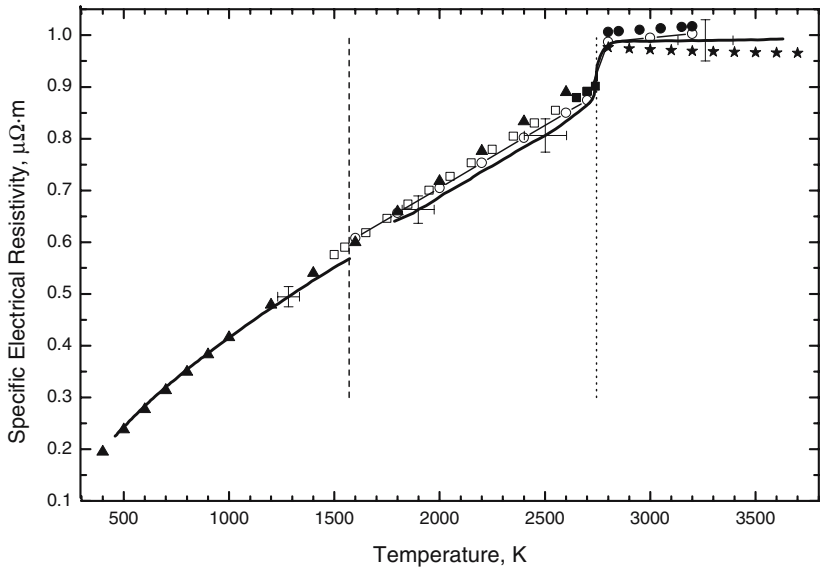

Fig. 4. Electrical resistivity of niobium (with initial geometry) versus temperature. Bold solid lines represent measured data from this work; vertical dashed line: end of values measured and calculated with DSC data (1570 K); vertical dotted line: melting temperature (2745 K); filled triangles: values from Zinov'yev [16]; open squares: values from Cezairliyan [17]; line with open circles: values from Boboridis [18], filled squares: values from Cezairliyan [19]; filled circles: values from Cezairliyan and McClure [20]; and filled stars: values from Gallob et al. [15].

3.3. Titanium

The titanium wires from "Goodfellow Cambridge Ltd." with a purity of 99.6+% were used as received. For the DSC-measurements we used the wire and additional cut samples from a plate of titanium.

In Fig. 5 the enthalpy versus temperature results for titanium are presented.

In the temperature range from $473\,\mathrm{K} < T < 1370\,\mathrm{K}$, we obtain from our DSC-measurements the following fits: (14)

$$H(T) = -187.758 + 0.607T, \quad (473\,K < T < 880\,K) \tag{14a}$$

$$H(T) = 358.284 + 0.639T + 7.134 \times 10^{-4}T^2, \quad (880\,K < T < 1090\,K) \tag{14b}$$

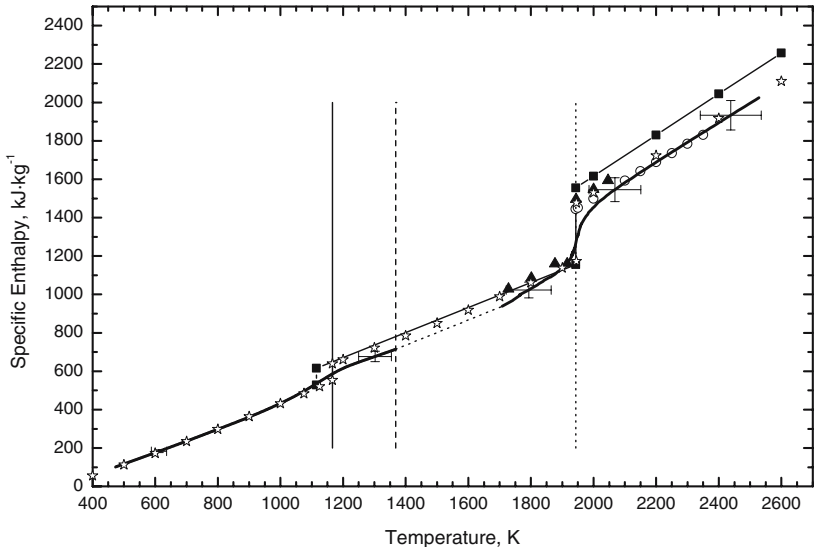

Fig. 5. Specific enthalpy versus temperature for titanium. Bold solid lines represent measured data from this work; vertical solid line: temperature of the $\alpha \rightarrow \beta$ transformation (1166 K) from Cezairliyan and Miiller [21]; vertical dashed line: end of values measured and calculated with DSC data (1368 K); vertical dotted line: melting temperature (1943 K); open stars: recommended values from Desai [22]; solid line with filled squares: values from Seydel et al. [8]; filled triangles: values from Berezin et al. [23]; open circles: literature values from Treverton and Margrave [24]; and dotted line: linear interpolation between DSC and pulse-heating values.

$$H(T) = -2917.626 + 5.127T - 1.820 \times 10^{-3} T^2, \quad (1090\,K < T < 1250\,K) \tag{14c}$$

$$H(T) = -62.831 + 0.568T, \quad (1250\,K < T < 1370\,K) \tag{14d}$$

The linear fit for solid titanium in the temperature range 1700 K $<$ $T <$ 1943 K obtained by pulse heating is

$$H(T) = -769.969 + T, \tag{15}$$

and for the liquid in the temperature range 1943 K $< T <$ 2500 K we obtain

$$H(T) = -608.296 + 1.043T. \tag{16}$$

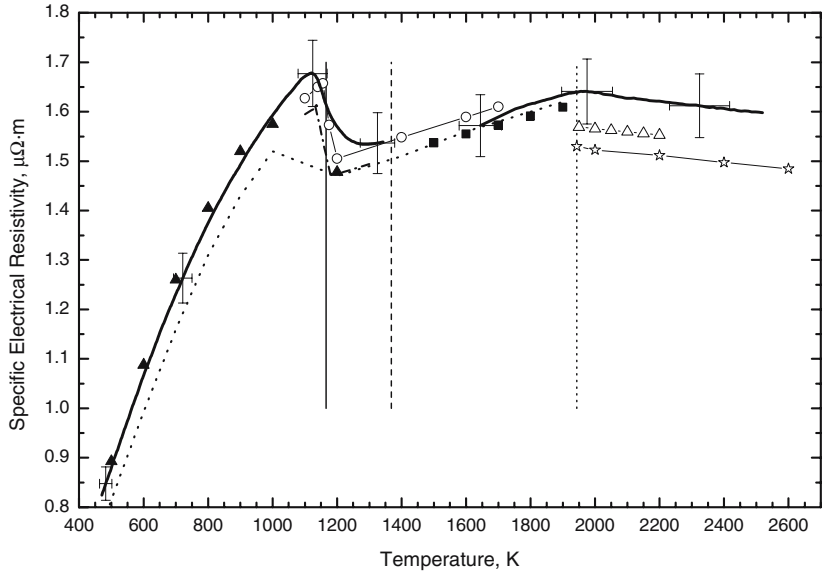

Fig. 6. Electrical resistivity of titanium (with initial geometry) versus temperature. Bold solid line represents measured data from this work; vertical solid line: temperature of the $\alpha \rightarrow \beta$ transformation (1166 K) from Cezairliyan and Miiller [21]; vertical dashed line: end of values measured and calculated with DSC data (1368 K); vertical dotted line: melting temperature (1943 K); dotted line: values from Zinov'yev [16] of polycrystalline titanium; filled triangles: values from Zinov'yev [16] of a single crystal titanium (||c); dotted-dashed line: values from Cezairliyan and Miiller [21]; line with open circles: values from Arutyunov et al. [25]; filled squares: values from Cezairliyan and Miiller [26] in the solid phase, line with open triangles: values from Boboridis [18]; and line with open stars: values from Seydel et al. [8].

Figure 6 depicts the electrical resistivity versus temperature results for titanium. In the range $473\,\mathrm{K} < T < 1130\,\mathrm{K}$ by means of DSC we obtain

$$\rho_{\mathrm{el,IG}}(T) = -0.382 + 3.070 \times 10^{-3} T - 1.098 \times 10^{-6} T^2, \tag{17}$$

and in the range from $1130\,\mathrm{K} < T < 1340\,\mathrm{K}$,

$$\rho_{\mathrm{el,IG}}(T) = 58.590 - 1.298 \times 10^{-1} T + 9.841 \times 10^{-5} T^2 - 2.485 \times 10^{-8} T^3. \tag{18}$$

By pulse heating we obtain in the solid range $1640\,\mathrm{K} < T < 1943\,\mathrm{K}$,

$$\rho_{\mathrm{el,IG}}(T) = 1.282 + 1.850 \times 10^{-4} T, \tag{19}$$

and in the liquid range from $1943\,\mathrm{K} < T < 2500\,\mathrm{K}$

$$\rho_{\mathrm{el,IG}}(T) = 1.794 - 7.830 \times 10^{-5} T. \tag{20}$$

4. DISCUSSION

The measured values for tungsten show very good agreement with literature values for the solid and liquid phases within the estimated uncertainties. The calculated values from a thermodynamic model from Gustafson et al. [7] are shown in comparison to our experimental data. We obtain a value of $(315 \pm 25)\,\mathrm{kJ\,kg^{-1}}$ for the enthalpy of fusion ΔH while Gustafson et al. calculate $285\,\mathrm{kJ\,kg^{-1}}$. The experimental value from Seydel et al. [8] is $264\,\mathrm{kJ\,kg^{-1}}$.

At the onset of melting (3687 K), which is indicated by a vertical dotted line in Fig. 2, we obtain a value of $1.10\,\mu\Omega\,\mathrm{m}$ for the electrical resistivity of tungsten, and at the end of melting, a value of $1.18\,\mu\Omega\,\mathrm{m}$; thus, an increase of $\Delta\rho_{IG} = 0.08\,\mu\Omega\,\mathrm{m}$ at melting is observed. In the solid phase the literature data from Goldsmith et al. [9], Zhorov [10], and Hust and Giarratano [11] are identical with the measured values within the estimated uncertainties. Also, the values from Seydel et al. [8] show the same trend in the liquid phase. When volume expansion is taken into account for resistivity, we obtain a value of $1.39\,\mu\Omega\,\mathrm{m}$ whereas Seydel et al. report $1.355\,\mu\Omega\,\mathrm{m}$ at the melting temperature. Differences in the electrical resistivity can also occur if the change of emissivity during the heating is taken into account. For data evaluation of the presented paper, a constant emissivity is assumed. For details about these changes of the electrical resistivity in tungsten, see Seifter [27]. Tungsten was the only material where we compared the measured resistivity results to literature values for the initial geometry and with volume expansion considered. All measured values show good agreement with literature values.

For solid niobium the measured results also show good agreement with literature values. As shown in Fig. 3 we obtain a value of $(795 \pm 32)\,\mathrm{kJ\,kg^{-1}}$ for the enthalpy H at the solidus and $(1150 \pm 46)\,\mathrm{kJ\,kg^{-1}}$ at the liquidus with the given fits extrapolated to the melting temperature. Kirillin et al. [13] report $817\,\mathrm{kJ\,kg^{-1}}$ for the onset of melting. We calculate a value of $(355 \pm 29)\,\mathrm{kJ\ kg^{-1}}$ for the heat of fusion ΔH while Hultgren et al. [12] recommend $284\,\mathrm{kJ\,kg^{-1}}$ and Sheindlin et al. [14] report $331\,\mathrm{kJ\,kg^{-1}}$.

At the onset of melting, which is indicated with a vertical dotted line in Fig. 4, we obtain a value of $0.87\,\mu\Omega\,\mathrm{m}$ for the electrical resistivity of niobium, and at the end of melting, a value of $0.99\,\mu\Omega\,\mathrm{m}$, thus, an increase of $\Delta\rho_{\mathrm{IG}} = 0.12\,\mu\Omega\,\mathrm{m}$ at melting is observed. Boboridis [18] reports a resistivity at the beginning and at the end of melting of 0.875 and $0.985\,\mu\Omega\,\mathrm{m}$, respec-

tively. All literature data for the liquid phase are in agreement with the results reported here, within the estimated uncertainties.

Titanium shows a $\alpha \rightarrow \beta$ phase transformation, which is indicated by a vertical solid line in Fig. 5. Phase transitions can easily be observed with DSC measurements, but can be partially or completely suppressed under pulse-heating conditions as applied within this experiment, due to the extreme high heating rates of $10^8\,\mathrm{K s^{-1}}$. As a result, enthalpy values in the solid phase (starting from the phase transition) are constantly lower than the literature values until the melting temperature is reached. We obtained a enthalpy of fusion ΔH of $(245 \pm 10)\,\mathrm{kJ\,kg^{-1}}$, Desai [22] recommends $(304 \pm 11)\,\mathrm{kJ\,kg^{-1}}$, Berezin et al. [23] report $(315 \pm 11)\,\mathrm{kJ\,kg^{-1}}$, and Seydel et al. [8] report $(399 \pm 8)\,\mathrm{kJ\,kg^{-1}}$. For the liquid phase our results show good agreement with the data of Treverton and Margrave [24], and the recommended values from Desai [22] as can be seen in Fig. 5.

The resistivity of titanium shows a maximum near the phase transition as shown in Fig. 6. After this phase transition a linear increase to the melting point is observed. At the melting point, which is indicated by a vertical dotted line, we obtain a value of $1.64\,\mu\Omega\,\mathrm{m}$ for the electrical resistivity of titanium. As opposed to tungsten and niobium, there is no erratic increase of the electrical resistivity at the end of melting. In the liquid phase our data are about 4% and 7% higher then the values of Boboridis [18] and Seydel et al. [8], respectively.

5. UNCERTAINTY

According to the guide to the expression of uncertainty in measurements (GUM) [28] uncertainties reported here are expanded relative uncertainties with a coverage factor of $k = 2$. An evaluated set of uncertainties is given; for the measured pulse-heating data the following uncertainties are estimated: current, I, 2%; voltage drop, U, 2%; temperature, T, 4%; mass m, 2%, from which we obtain for enthalpy, H, 4%; enthalpy of fusion ΔH, 8%; specific heat capacity c_p, 8%, specific electrical resistivity with initial geometry, $\rho_{\mathrm{el,IG}}$, 4%, and specific electrical resistivity with volume expansion considered, $\rho_{\mathrm{el,VOL}}$ 6%. The corresponding expanded uncertainties are indicated on the figures.

For the DSC data the uncertainties are given by: temperature, T, 2 K and specific heat capacity, c_p, 3%.

The uncertainties of the temperature values after the merging of pulse-heating and DSC data results are dominated by the uncertainty of the enthalpy values obtained by pulse heating. Based on this, the uncertainty over the whole temperature interval in Figs. 2, 4, and 6 is estimated as 4%.

6. CONCLUSION

In this study the temperature dependences for the enthalpy and electrical resistivity of tungsten, niobium, and titanium are reported and compared to literature values. The temperature dependences could be extrapolated down to a temperature of about 500 K. Despite the different heating rates, both methods show very good agreement of the obtained thermophysical data within the stated uncertainties of each experiment.

ACKNOWLEDGMENT

This work was supported by the Fonds zur Förderung der wissenschaftlichen Forschung (FWF), Vienna, Austria under contract No. P15055.

REFERENCES

1. G. Pottlacher, H. Jäger, and T. Neger, *High Temps.-High Press*. **19:**19 (1987).
2. C. Cagran, C. Brunner, A. Seifter, and G. Pottlacher, *High Temps. High. Press.* **34**:669 (2002).
3. B. Wilthan, C. Cagran, and G. Pottlacher, *Int. J. Thermophys*. **25**:1519 (2004).
4. G. Pottlacher, E. Kaschnitz, and H. Jäger, *J. Phys.: Condens Matter* **3**:5783 (1991).
5. C. Cagran, B. Wilthan, and G. Pottlacher, *Int. J. Thermophys* **25**:1551 (2004).
6. R. Bedford, G. Bonnier, H. Maas, and F. Pavese, *Metrologia* **33**:133 (1996).
7. P. Gustafson, *Int. J. Thermophys*. **6**:395 (1985).
8. U. Seydel, W. Fucke, and H. Wadle, *Die Bestimmung thermophysikalischer Daten flüssiger hochschmelzender Metalle mit schnellen Pulsaufheizexperimenten*, Wissenschaftlicher Fachverlag Düsseldorf, Düsseldorf (1980).
9. A. Goldsmith, T. Waterman, and H. Hirschhorn, *Handbook of Thermophysical Properties of Solid Materials*, Vol. 1 (Pergamon Press, Oxford, 1961).
10. G. Zhorov, *High Temperature* **10**:1202–1204 (1972), Translated from *Teplofizika Vysokikh Temperatur* **10**: 1332–1334, Moscow (1972).
11. J. Hust and P. Giarratano, *Standard Reference Materials: Thermal Conductivity and Electrical Resistivity Standard Reference Materials: Tungsten SRM's 730 and 799, from 4 to 3000 K*, Natl. Bur. Stand., Boulder, Colorado (1975).
12. R. Hultgren, P. D. Desai, D. T. Hawkins, M. Gleiser, K. K. Kelley, and D. D. Wagman, *Selected Values of the Thermodynamic Properties of the Elements*, American Society for Metals, UMI, Reprinted (1990).
13. V. Kirillin, A. Sheindlin, V. Chekhovskoi, and I. Zhukova, *High Temperature* **3**:357 (1965); Translated from *Teplofizika Vysokikh Temperatur* **3**:395, Moscow (1965).
14. A. Sheindlin, B. Ya Berezin, and V. Ya Chekhovskoi, *High Temps.-High Press*. **4:**611 (1972).
15. R. Gallob, H. Jäger, and G. Pottlacher, *High Temps.-High Press*. **17:**207 (1985).
16. V. E. Zinov'yev, *Metals at High Temperatures-Standard Handbook of Properties*, National Standard Reference Data Service of the USSR (Hemisphere, New York, 1990).
17. A. Cezairliyan, *J. Res. Natl. Bur. Stand. (U.S.)* **75A:**565 (1971).

18. K. Boboridis, *Application of Single-Wavelength Radiation Thermometry and High-Speed Laser Polarimetry to Thermophysical Property Measurements on Pulse-Heated Metals* (Ph. D. Thesis, TU-Graz, Austria (http://iep.tugraz.at), 2001).
19. A. Cezairliyan, *High Temps.-High Press*. **4:**453 (1972).
20. A. Cezairliyan and J. McClure, *Int. J. Thermophys.* **8**:803 (1987).
21. A. Cezairliyan and A. Miiller*J. Res. Natl. Bur. Stand. (U.S.)* **83:**127 (1978).
22. P. Desai, *Int. J. Thermophys*. **8**:781 (1987).
23. B. Berezin, S. Kats, M. Kenisarin, and V. Chekhovskoi, *High Temperature* **12**:450 (1974); Translated from*Teplofizika Vysokikh Temperatur* **12**:524, Moscow (1973).
24. J. Treverton and J. Margrave, *J. Chem. Thermodyn.* **3**:473 (1971).
25. A. Arutyunov, S. Banchila, and L. Filippov, *High Temperature* **9**:487 (1971), Translated from *Teplofizika Vysokikh Temperatur* **9**:535, Moscow (1970).
26. A. Cezairliyan and A. Miiller, *High Temps.-High Press*. **9:**319 (1977).
27. A. Seifter, *Ph. D. Thesis* (TU-Graz, Austria (http://iep.tugraz.at), 2001).
28. Expression of the Uncertainty of Measurement in Calibration, EA-4/02, http://www.european-accreditation.org/pdf/EA-4-02ny.pdf (1999).